Japanese Journal of Veterinary Research 69(2): 125-134, 2021

JJVR

REGULAR PAPER Experimental Research

Effects of gel pad thickness on skin stiffness evaluation by ultrasonographic strain elastography in normal dogs

Sothavy Chhay[1)], Kiwamu Hanazono[2,3,*)], Jo Kitahara[1)], Ai Hori[3)], Kenjiro Miyoshi[1,3)], Takaharu Itami[1,3)], Daiji Endoh[2)] and Tetsuya Nakade[1,3)]

[1)] Department of Small Animal Clinical Sciences, School of Veterinary Medicine, Rakuno Gakuen University, 582 Bunkyodai Midorimach, Ebetu-shi, Hokkaido 069-8501, Japan
[2)] Department of Biosciences, School of Veterinary Medicine, Rakuno Gakuen University, Ebetsu, Hokkaido 069-8501, Japan
[3)] Animal Medical Center, Rakuno Gakuen University, 582 Bunkyodai Midorimach, Ebetu-shi, Hokkaido 069-8501, Japan

Received for publication, November 8, 2020; accepted, February 25, 2021

Abstract

Gel pads are commonly used for skin ultrasound examination; however, the effect of their thickness on the measured values is unknown. We investigated the effect of pad thickness on skin stiffness measurement in healthy dogs. The skin stiffness of the dorsal neck was measured using a durometer. Ultrasonographic strain elastography was performed with 5-, 10-, and 20-mm-thick pads. Among the strain ratios, muscle/skin (5 mm) showed a significantly positive correlation with skin stiffness. In the strain histogram, AREA (20 mm), CONTRAST (20 mm), MEAN (5, 20 mm), and STANDARD DEVIATION (20 mm) were significantly correlated with skin stiffness. In conclusion, the thickness of the gel pad affects the measurements during skin ultrasonographic strain elastography.

Key Words: Gel pad, normal dog, skin ultrasonography, ultrasonographic strain elastography

Introduction

Skin ultrasonography was first used in human medicine[2)] and has been widely used since then as a non-invasive and convenient technique to diagnose cutaneous neoplasia[5,7)] and inflammatory skin diseases[8,21,26)]. This technique can also be used in veterinary medicine and has been reportededly useful for the diagnosis of cutaneous hemangiosarcoma and lymphangioma in horses[23,16)].

In human medicine, the relationship between skin stiffness and various skin diseases, such as inflammatory and neoplastic diseases, has been investigated[9,24,28,30)]. One non-invasive method for evaluating skin stiffness is the durometer[13)]. The durometer is constructed as follows: a push needle protrudes from the pressure surface of the durometer's body, which is internally connected to a spring. Measurement is performed by pressing the push needle and pressure surface against the specimen's surface, causing the push needle to

* Corresponding author: Kiwamu Hanazono DVM, PhD
Address: Department of Basic Veterinary Medicine, School of Veterinary Medicine, Rakuno Gakuen University, Ebetsu, Hokkaido 069-8501, Japan
Tel: +81-11-388-4808, Fax: +81-11-386-4808, E-mail: k-hanazono@rakuno.ac.jp
doi: 10.14943/jjvr.69.2.125

press into and deform the specimen with the force of the spring, which in turn generates a repulsive force in the specimen. When the pressure and repulsive force are in equilibrium, the needle's depth of indentation is indicated as stiffness, using a range of 0 to 100 points; however, there is no physical unit for this. In human medicine, durometric measurements of the skin are highly correlated with skin stiffness[3], which is why durometers are widely used to assess the severity of systemic scleroderma[24,28].

Ultrasonographic strain elastography is a technique for imaging the relative displacement (strain) of tissue caused by the compression of the probe to determine tissue stiffness[18]. The basic material property evaluated by strain elastography is the elasticity of a material, described as the tendency of a material to resume its original size and shape after being subjected to a deforming force or stress. This change in size and shape is known as the strain[17]. Good elastograms can be obtained by generating sufficient strain in the region of interest (ROI), for which sufficient stress must be applied[11].

In human medicine, ultrasonographic strain elastography has been evaluated as a method for differentiating between benign and malignant skin tumors[9,30]. Meanwhile, strain ratios have been used for various types of evaluations in human medicine such as diagnosis of breast cancer[25,40], pancreatic mass evaluation[22], classification of liver fibrosis[29,37], and prediction of optimal biopsy targets in prostate cancer diagnosis[39]. Additionally, strain ratios have also been used in diagnostic studies of human skin tumors, with malignant lesions showing a higher strain ratio (healthy skin/lesion) since they are typically harder than normal tissue[9]. A strain histogram can extract 11 kinds of texture features by using the histogram display function in the ROI of the elastogram and texture analysis using the gray level co-occurrence matrix[19]. Several human medical studies have attempted to infer the tissue structure and stiffness of the liver, thyroid, and skin using these texture features[15,29,30,38].

In skin ultrasonography, a gel pad (i.e., standoff pad) is often used to clearly delineate the body surface and superficial layers. This is because the gel pad does not contain scatterers and is a medium that shows the skin structure by its adhesion to the skin and probe[20,30,35]. The usefulness of gel pads has been demonstrated for the evaluation of the body surface. The gel pads improved the visualization in cases where the vocal cords were difficult to observe due to calcification of the thyroid gland[36]. In ultrasonographic strain elastography, gel pads are also expected to normalize the applied pressure and improve the image quality of the skin surface[10,20,35]. However, the appropriate thickness of the gel pad for skin ultrasonographic strain elastography is not certain.

Our hypothesis is that the measurements obtained by strain ratio and strain histogram indicate skin stiffness; however, we speculate that the differences in the gel pad thickness may affect these measurements. The purpose of this study is to assess skin stiffness by ultrasonographic strain elastography with gel pads of various thicknesses, as well as to investigate how the thickness of the gel pad affected these assessments in dogs.

Materials and Methods

Animals

Our study was performed with 10 beagles: four intact females and six intact males. The age range was 5-9 years and body weight range was 9.0-13.1 kg. All dogs were considered clinically healthy based on the results of a clinical examination. The study design was approved by the Rakuno Gakuen University Animal Experiment Committee (Approval number: VH19B8). The dogs were held in the prone position, and all examinations were performed without sedation or anesthesia.

Fig. 1.
Attachment of the gel pad and application of the probe. The gel pad is attached to the probe at the tip and covered with a condom. Subsequently, the probe with the attached gel pad is placed on the skin of the neck without vibration.

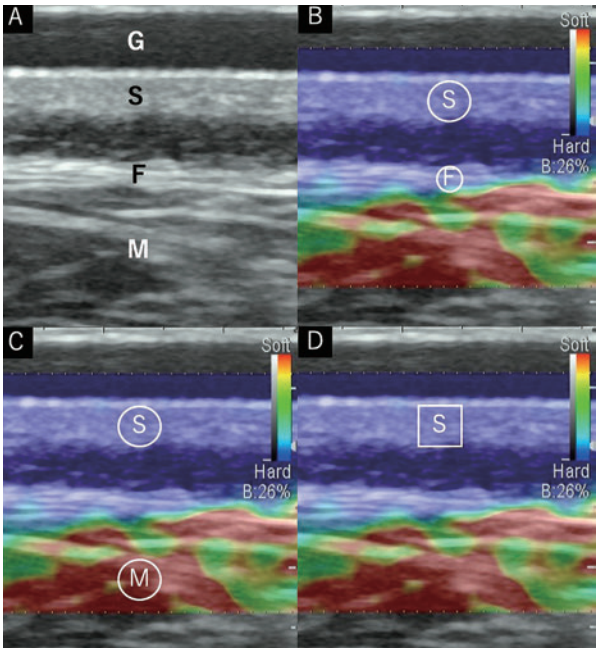

Fig. 2.
Skin structure on B-mode image (A) and ROI settings for fat/skin strain ratio (B), muscle/skin strain ratio (C), and strain histogram (D) on elastogram. A circular ROI was used for the strain ratio (B, C) and a square ROI was used for the strain histogram(D).
(A)The epidermis of the skin is the most superficial layer of the body and presents as a granular hyperechoic layer. The subcutaneous fat (F) is located beneath the skin and is observed as a multilayered hyperechoic layer. The muscle (M) lies below the subcutaneous fat and is hypoechoic. Gel pad (G) is observed as a uniform hypoechoic layer at the top of the image.
(B)In fat/skin strain ratio, the ROI of the skin (circular "S") and the ROI of the fat (circular "F") were set in the epidermis of the skin and subcutaneous fat, respectively.
(C)In muscle/skin strain ratio, the ROI of the muscle (circular "M") was set in the muscle. The ROI of the skin (S) was set in the same way as with fat/skin.
(D)The ROI for the strain histogram (quadrangle "S") was set in the epidermis only without comparison.

Measurement of skin stiffness by the measuring devices

Before ultrasonographic examination, the stiffness of the skin in all dogs was measured using a durometer (Digital Hardness tester type C, tip stroke: 0-2.5 mm; Euhong, China, Dayirenn). First, the dorsal neck region was shaved with a clipper and a 2-cm straight line was marked on the skin with a permanent marker pen. The durometer was used to measure skin stiffness of the neck region where the hair had been shaved. The durometer was carefully held and stabilized on the surface of the skin, and the measured values appeared as digital numbers (stiffness), which were then recorded. The stiffness was measured three times at one point on the marked line.

Ultrasonographic strain elastography

Ultrasound images were obtained with an imaging system (ARIETTA70; Hitachi, Japan, Tokyo) in which the dogs were held in sternal recumbency and the dorsal neck skin was visualized using a 13-MHz linear probe (L64; Hitachi, Japan, Tokyo). Ultrasonographic strain elastography images were scanned three times using the same transducer with 5-, 10-, or 20-mm-thick pads (Echo Gel Pad; Yasojima, Japan, Kobe). The acoustic impedance and damping rate of these gel pads were 1.42×10^6 Pa·s/m and 3.5 dB/cm at a frequency of 5 MHz, respectively. The 5-, 10-, and 20-mm-thick pads were cut to fit the probe surface and were covered with a condom together with the probe (Fig. 1).

Table 1. Correlation between the strain ratios in each condition and skin stiffness values measured with a durometer

Strain ratio	Gel pad	Mean	SD	Median	Range	r	p-value
fat/skin	5 mm	3.12	1.97			0.110	0.763
	10 mm	2.67	4.72			-0.105	0.773
	20 mm	2.51	1.95			0.182	0.615
muscle/skin	**5 mm**			**9.23**	**7.75 - 22.19**	**0.745**	**0.026**
	10 mm			7.34	2.16 - 29.17	-0.252	0.449
	20 mm			5.49	1.53 - 26.17	-0.117	0.726

*SD: Standard deviation for each measurement

Table 2. Correlation between the strain histogram parameters in each condition and skin stiffness values measured with a durometer

Strain histogram	Gel pad	Mean	SD*	Median	Range	r	p-value
MEAN	**5 mm**			**25.79**	**17.40 - 49.60**	**-0.696**	**0.037**
	10 mm	29.08	18.03			-0.391	0.264
	20 mm	**34.54**	**19.86**			**-0.725**	**0.018**
STANDARD DEVIATION	5 mm	13.81	6.39			-0.578	0.080
	10 mm			19.11	5.10 - 30.24	-0.217	0.548
	20 mm	**20.06**	**12.19**			**-0.813**	**0.004**
AREA(%)	5 mm			97.03	71.00 -100.0	0.314	0.346
	10 mm			92.26	57.01-100.0	0.106	0.788
	20 mm			**93.86**	**54.66 - 100.0**	**0.704**	**0.035**
COMPLEXITY	5 mm			15.87	14.94 - 21.61	-0.511	0.125
	10 mm			15.57	15.21 - 21.02	-0.068	0.839
	20 mm			15.40	14.53 - 21.16	-0.419	0.209
SKEWNESS	5 mm			0.69	-0.06 - 1.79	0.062	0.854
	10 mm	0.94	0.62			0.445	0.198
	20 mm	0.95	0.57			0.112	0.759
KURTOSIS	5 mm			2.80	2.15 - 6.10	0.111	0.740
	10 mm	3.80	1.62			0.350	0.321
	20 mm			3.52	1.93 - 6.09	0.197	0.555
CONTRAST	5 mm			1.98	0.50 - 18.24	-0.289	0.386
	10 mm	13.37	12.80			0.046	0.899
	20 mm			**8.16**	**0.61- 44.21**	**-0.720**	**0.031**
ENTROPY	5 mm	1.99	0.26			-0.356	0.312
	10 mm	2.05	0.46			-0.238	0.508
	20 mm	2.13	0.50			-0.599	0.068
INVERSE DIFFERENCE MOMENT	5 mm	0.64	0.08			0.448	0.194
	10 mm			0.62	0.38 - 0.80	0.019	0.956
	20 mm			0.51	0.27 - 2.21	0.529	0.112
ANGULAR SECOND MOMENT	5 mm			0.04	0.02 - 0.30	0.259	0.438
	10 mm			0.02	0.00 - 0.22	0.012	0.971
	20 mm			0.04	0.00 - 0.33	0.160	0.631
CORRELATION	5 mm	0.99	0.01			0.039	0.915
	10 mm			0.99	0.96 - 1.00	-0.326	0.328
	20 mm			0.99	0.97 - 1.53	0.049	0.883

*SD: Standard deviation for each measurement

We used the "minimal compression" method to obtain the vibration for ultrasonographic strain elastography[4]. In this method, the probe is placed perpendicular to the skin without conscious shaking and minimal pressure is applied. This method detects vibrational energy from both the vibrations caused by involuntary muscle contraction of the examiner's hand as well as the vibrations caused by the animals' muscle contraction, and since the image does not move

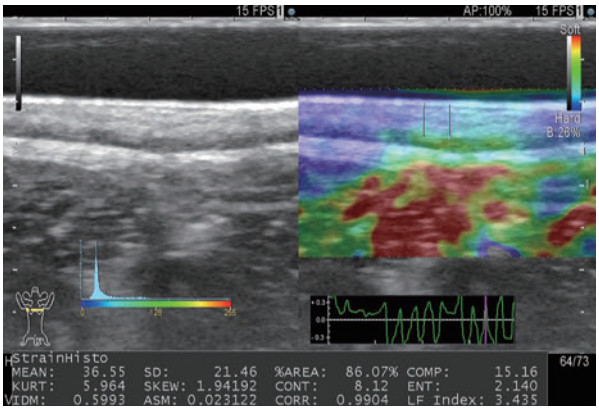

Fig. 3.
Strain histogram image. The B-mode image and histogram (bottom) are shown on the left of the screen, and the elastogram and strain graph are shown on the right. The bottom part of the screen shows each calculated feature.

at all, extremely detailed images can be obtained. For appropriate vibration, we checked the strain graph displayed on the screen and applied only data in the range of -0.3 to 0.31).

A circular ROI was selected for the skin, subcutaneous fat, and muscle for the strain ratio evaluation. Subcutaneous fat-to-skin ratio (fat/skin) and muscle-to-skin ratio (muscle/skin) were calculated (Fig. 2). The pixel values were shown in 256 color gradients according to the color mapping from blue (0) to red (255). The scale ranged from blue for the hardest component with the lowest strain to red for the softest component with the highest strain. For the strain histogram, a rectangular ROI was selected for the skin area (Fig. 2). The quantifiable characteristics of the strain histogram include the mean of the relative strain values (MEAN) and standard deviation of the relative strain values (STANDARD DEVIATION), area of low strain (AREA), complexity of the low strain area (COMPLEXITY), kurtosis of the strain histogram (KURTOSIS), skewness (SKEWNESS), contrast (CONTRAST), entropy (ENTROPY), inverse difference moment (INVERSE DIFFERENCE MOMENT), angular second moment (ANGULAR SECOND MOMENT), and correlation (CORRELATION) for the gray level co-occurrence matrix. These parameters were automatically calculated by the ultrasound system (Fig. 3).

MEAN is the mean value of the relative strain values in the ROI, and a small value indicates that a large number of hard regions were included. STANDARD DEVIATION is the standard deviation of the relative strain values in the ROI, and evaluates the variation in the strain values. AREA is the ratio of the area of the low strain regions, which increases as the number of low strain regions increases. COMPLEXITY is defined as the average complexity of the low strain region, which indicates how complex the contour is in relation to the area of the low strain regions. SKEWNESS is used as a measure of asymmetry and its value indicates the extent to which symmetric objects in the histogram are distorted, while KURTOSIS is the spread from the mean on the histogram. For factors associated with the gray level co-occurrence matrix, CONTRAST indicates the feature of textual variation, ENTROPY indicates the feature of textual randomness, INVERSE DIFFFERENCE MOMENT indicates the feature of textual homogeneity, ANGULAR SECOND MOMENT indicates the feature of textual homogeneity, and CORRELATION indicates the feature of textual directionality[15,19,38]. All elastography parameters were measured three times, and the average values were calculated.

Statistical analysis

The obtained data were analyzed using a free statistical software (R, a language and environment for statistical computing, version 3.6.0, R Foundation for Statistical Computing, Vienna, Austria) for the Shapiro-Wilk normality test and commercially available software (Statmate III, ATMS, Tokyo, Japan) for the Pearson's correlation coefficient, Spearman's rank correlation coefficient, one-way analysis of variance, and the Kruskal–Wallis test.

If the measurements showed a normal distribution, the mean and standard deviation (SD) of the measurements were obtained; if they did not show a normal distribution, the median

of the measurements and range were obtained. A parametric test was used for comparing data that followed a normal distribution, whereas a non-parametric test was used for comparing data that did not follow a normal distribution.

To determine the correlation between the values measured by the durometer and values measured by ultrasound elastography, we used Pearson's correlation coefficient (parametric test) or Spearman's rank correlation coefficient (non-parametric test). One-way analysis of variance (parametric test) or Kruskal–Wallis test (non-parametric test) were used to determine significant differences among the gel pads. A p value of < 0.05 was considered significant.

Results

The mean skin stiffness value measured with the durometer in the 10 dogs was 8.98 ± 0.87 points (mean±SD). The ultrasound elastography images for each gel pad are shown in Fig. 3. Elastograms with inadequate colorization in the ROI were found in 36.67% of under 5 mm, 50% of under 10 mm, and 90% of under 20 mm thick pads. Table 1 shows the strain ratios and correlation between the strain ratios and skin stiffness. The muscle/skin ratio demonstrated a significantly positive correlation with skin stiffness for the under 5-mm-thick pad ($r = 0.745$, $p = 0.026$). However, the fat/skin ratio did not correlate with skin stiffness for any of the pads. The correlations between the strain histogram and skin stiffness are shown in Table 2. According to the results, AREA (20 mm: r=-0.704 p=0.035), CONTRAST (20 mm: r=-0.720, p=0.031), MEAN (5 mm: r=-0.696, p=0.037; 20 mm: r=-0.725, p=0.018), and STANDARD DEVIATION (20 mm: r=-0.813, p=0.004) showed significant correlations with skin stiffness. The greatest number of correlations were found with the 20-mm-thick pad. No significant difference was found between the gel pads for any of the ultrasound elastography values.

Discussion

In this study, the muscle/skin ratio with a 5-mm-thick pad showed a significantly positive correlation with skin stiffness, while the muscle/skin ratios with the other pads demonstrated no correlation. Strain elastography was performed with the transducer compressed perpendicular to the skin surface; this approach requires stable pressure or stable compression by the operator to maintain the good quality of elastography[31]. As the thickness of the gel pad increased, there was an increasing trend in the percentage of images with uncolored areas indicating insufficient stress deep in the muscle of the ROI. In general, gel substances have a shock-absorbing effect14). As the thickness of the gel pad increases, it may result in the generation of less-than-optimal stress in the deep region. Moreover, if these gel pads were cut to fit the width of the probe, they may undergo buckling, thus generating insufficient stress.

In breast elastography, fat tissue has been used as a comparator for lesions (FLR: fat-to-lesion strain ratio) [31]. However, in this study, no significant correlation was found between the fat/skin ratio and skin stiffness. Ambroziak et al.[3] reported that the subcutaneous tissue contains a mixture of soft distorted adipose tissue and hard less distorted connective tissue, which makes the distortions less homogeneous. It also reduces the reproducibility of ultrasound elastography in cases with thick layers of fat[3]. Therefore, the lack of a significant correlation between the fat/skin ratio and skin stiffness in the present study may be due to the inconsistent distortion of the adipose part of the subcutaneous tissue.

In a study of human skin tumors, MEAN was the most direct measure of strain within the lesion as a diagnostic parameter[30]. In addition, Morikawa et al. found in a study of liver fibrosis that liver stiffness showed a negative correlation with the MEAN, while showing positive correlations with the AREA, STANDARD DEVIATION, and COMPLEXITY[30]. In this study,

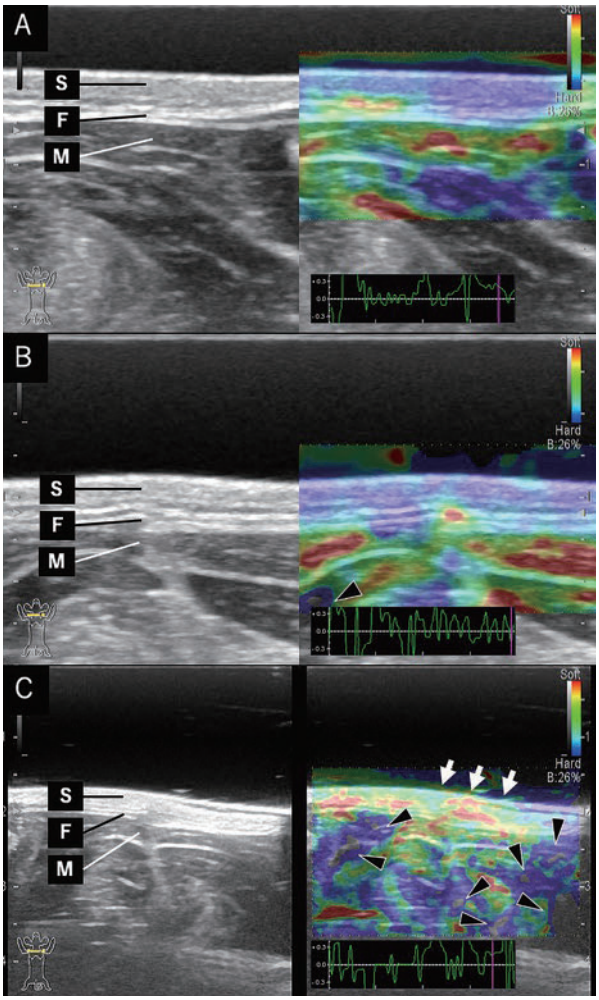

Fig. 4.
Ultrasonographic strain elastography image of the dorsal neck skin under a 5-mm-thick pad (A), 10-mm-thick pad (B), and 20-mm-thick pad (C). Areas of the skin (S), fat (F), and muscle (M) are indicated by bars. Under the 5-mm-thick pad, almost the entire ROI is colorized; however, non-colored areas (arrowhead) are seen locally under the 10-mm-thick pad with multiple areas under the 20-mm-thick pad. The skin area tends to appear bluer and more uniform under the 5- and 10-mm-thick pads than under the 20-mm-thick pad (A-C). Under the 20-mm-thick pad (C), a slope is formed on the skin surface due to compression (arrow).

skin stiffness demonstrated negative correlations with the MEAN, STANDARD DEVIATION, and CONTRAST, while showing positive correlations with the AREA. The smaller the MEAN, the more hard regions are included in the ROI[15]. On the other hand, AREA indicates the area of the low strain regions in the ROI; therefore, it increases with an increase in the low strain regions. Consequently, an increase in the AREA indicates greater stiffness[15]. These facts support the finding that the MEAN decreases, and AREA increases, with increasing skin stiffness.

CONTRAST shows concentration differences in the texture features[19]; however, its clinical significance in the strain histogram is not clear[15,38]. In normal skin, skin stiffness is dependent on the water content, and as the water content decreases, skin stiffness increases[27,33,34]. Ceramides, as a component of the lipid matrix in the interstitium, play an important role in water retention in the epidermis, and their loss results in reduced water content of the skin[12]. It has been reported that the ceramide content of the skin varies among humans[32]. A decrease in skin hydration due to low ceramide content may increase skin stiffness, while a decrease in the interstitial components may reduce the concentration differences in the elastogram. However, since histological evaluation was not performed in the present study, we could not postulate the relationship between skin stiffness and tissue structure.

On the other hand, STANDARD DEVIATION, which was positively correlated with the liver stiffness in a previous report[29], showed a negative correlation with skin stiffness in our study. STANDARD DEVIATION has been reported to indicate tissue heterogeneity[15]. Morikawa et al. reported that liver fibrosis is characterized by an increase in the liver tissue stiffness and a concurrent increase in the stiffness variability, or STANDARD DEVIATION, as the fibrosis progresses[29]. Thus STANDARD DEVIATION was thought to be positively correlated with liver fibrosis. The present study used normal skin tissue, and the change in stiffness was not related to fibrosis. Therefore, the mechanism may be different from what has been reported previously. The reason for the negative correlation with STANDARD DEVIATION for the under 20-mm-thick pad may be that the harder the skin, the lower the absolute value of strain in the ROI, and the more difficult it is to recognize small areas of strain due to attenuation. Thus, STANDARD

DEVIATION showed a negative correlation with skin stiffness.

The most significant correlations were found for the under 20-mm-thick pad. However, there are no clear studies to support this result. The depth of the lesion has been reported to not affect the assessments with the strain histogram in breast tumors[6]. Conversely, it has been recommended that the ROI should be set at least 20 mm deeper than the liver coat because the liver surface appears hard (blue) in the strain histogram due to compression[29]. In fact, the 5-mm-and 10-mm-thick pads tended to show harder (blue) skin and higher AREA in this study (Table 2, Fig. 4). These results suggest that a 20 mm distance from the surface of the probe may be required to obtain the skin strain histogram using a gel pad in this condition. The extent to which the thickness of the gel pads correlated with skin stiffness was different for the strain ratio and strain histogram. The reason for this discrepancy may be the fact that the strain ratio is a relative assessment performed using deep muscle and fat as comparators, whereas the strain histogram is based on skin only.

The main limitation of this study is the small number of cases. Only 10 conscious beagle dogs were included in the study. Breed, age, sex, and muscle tension differences were not taken into account. In addition, we cannot completely guarantee that we were able to accurately measure skin stiffness because we were unable to develop a skin stiffness tester specifically for dogs and substituted a commercially available durometer. Likewise, we have not been able to fully determine the meaning of the strain histogram because we did not perform a histological examination of the skin. Moreover, the suitable gel pad thickness may also vary with the components of the gel pad and the ultrasound device. In addition, inter-examiner errors were not considered in this study. Therefore, it is not possible to completely determine the appropriate gel pad thickness based on the results of this study alone.

In conclusion, the thickness of the gel pad affects the measurements when performing skin ultrasonographic strain elastography.

Conflict of Interest Declaration

No third-party funding or support was received in connection with this study or for writing and publishing this manuscript. The authors declare no conflicts of interest.

Acknowledgements

The authors thank Ako Kakuta, Hisashi Ishiguro, and Kota Nagawa (Unit of Veterinary Diagnostic Imaging, Rakuno Gakuen University) for their cooperation and support.

References

1) Akagi R, Chino K, Dohi M, Takahashi H. Relationships between muscle size and stiffness of the medial gastrocnemius at different ankle joint angles in young men. Acta Radiol 53, 307-311, 2012.
2) Alexander H, Miller DL. Determining skin thickness with pulsed ultrasound. J Invest Dermatol 72, 17-19, 1979.
3) Ambroziak M, Pietrusk P, Noszczyk B, Paluch T. Ultrasonographic elastography in the evaluation of normal and pathological skin - a review. Postepy Dermatol Alergol 36, 667-672, 2019.
4) Barr RG. Breast elastography, Thieme Medical Publishers, New York, pp.10-27, 2014.
5) Bhatt KD, Tambe SA, Jerajani HR, Dhurat RS. Utility of high-frequency ultrasonography in the diagnosis of benign and malignant skin tumors. Indian J Dermatol Venereol Leprol 83, 162-182, 2017.
6) Carlsen JF, Ewertsen C, Sletting S, Talman ML, Vejborg I, Bachmann Nielsen M. Strain

histograms are equal to strain ratios in predicting malignancy in breast tumours. PLoS ONE 12, e0186230, 2017.
7) Catalano O, Roldán FA, Varelli C, Bard R, Corvino A, Wortsman X. Skin cancer: findings and role of high-resolution ultrasound. J Ultrasound 22, 423-431, 2019.
8) Ch'ng SS, Roddy J, Keen HI. A systematic review of ultrasonography as an outcome measure of skin involvement in systemic sclerosis. Int J Rheum Dis 16, 264-272, 2013.
9) Dasged B, Morris MA, Mehregan D, Siegel EL. Quantified ultrasound elastography in the assessment of cutaneous carcinoma. Br J Radiol 88, 20150344, 2015.
10) De Zordo T, Fink C, Feuchtner GM, Smekal V, Reindl M, Klauser AS. Real-time sonoelastography findings in healthy Achilles tendons. AJR Am J Roentgenol 193, W134-8, 2009.
11) Dietrich CF, Barr RG, Farrokh A, Dighe M, Hocke M, Jenssen C, Dong Y, Saftoiu A, Havre RF. Strain elastography - How to do it? Ultrasound Int Open 3, E137-149, 2017.
12) Draelos ZD. The science behind skin care: Moisturizers. J Cosmet Dermatol 17, 138-144, 2018.
13) Falanga V, Bucalo B. Use of a durometer to assess skin hardness. J Am Acad Dermatol 29, 47-51, 1993.
14) Fergason J, Smith DG. Socket considerations for the patient with a transtibial amputation. Clin Orthop Relat Res 361, 76-84, 1999.
15) Fujimoto K, Kato M, Kudo M, Yada N, Shiina T, Ueshima K, Yamada Y, Ishida T, Azuma M, Yamasaki M, Yamamoto K, Hayashi N, Takehara T. Novel image analysis method using ultrasound elastography for noninvasive evaluation of hepatic fibrosis in patients with chronic hepatitis C. Oncology 84, 3-12, 2013.
16) Gehlen H, Wohlsein P. Cutaneous lymphangioma in a young Standardbred mare. Equine Vet J 32, 86-88, 2000.
17) Gennisson JL, Deffieux T, Fink M, Tanter M. Ultrasound elastography: Principles and techniques. Diagn Inter Imaging 94, 487-495, 2013.
18) Ginat DT, Destounis SV, Barr RG, Castaneda B, Strang JG, Rubens DJ. US elastography of breast and prostate lesions. Radiographics 29, 2007-2016, 2009.
19) Haralick, RM, Shanmugam K, Dinstein I. Textural Features for Image Classification. IEEE Trans Syst Man Cybern 6, 610-621, 1973.
20) Hashemi HS, Fallone S, Boily M, Towers A, Kilgour RD, Rivaz H. Assessment of mechanical properties of tissue in breast cancer-related lymphedema using ultrasound elastography. IEEE Trans Ultrason Ferroelectr Freq Control 66, 541-550, 2019.
21) Hermann RC, Ellis CN, Fitting DW, Ho VC, Voorhees JJ. Measurement of epidermal thickness in normal skin and psoriasis with high-frequency ultrasound. Skin Pharmacol 1, 128-136, 1988.
22) Itokawa F, Itoi T, Sofuni A, Kurihara T, Tsuchiya T, Ishii K, Tsuji S, Ikeuchi N, Umeda J, Tanaka R, Yokoyama N. EUS elastography combined with the strain ratio of tissue elasticity for diagnosis of solid pancreatic masses. J Gastroenterol 46, 843-853, 2011.
23) Jean D, Lavoie JP, Nunez L, Lagacé A, Laverty S. Cutaneous hemangiosarcoma with pulmonary metastasis in a horse. J Am Vet Med Assoc 204, 776-778, 1994.
24) Kissin EY, Schiller AM, Gelbard RB, Anderson JJ, Falanga V, Simms RW, Korn JH, Merkel PA. Durometry for the assessment of skin disease in systemic sclerosis. Arthritis Rheum 55, 603-609, 2006
25) Kumm TR, Szabunio MM. Elastography for the characterization of breast lesions: initial clinical experience. Cancer Control 17, 156-161, 2010.
26) Marina ME, Botar Jid C, Roman II, Mihu CM, Tătaru AD. Ultrasonography in psoriatic disease. Med Ultrason 17, 377-382, 2015.
27) Mayrovitz HN, Corbitt K, Grammenos A, Abello A, Mammino J. Skin indentation firmness and tissue dielectric constant assessed in face, neck,

and arm skin of young healthy women. Skin Res Technol 23, 112-120, 2017.

28) Merkel PA, Silliman NP, Denton CP, Furst DE, Khanna D, Emery P, Hsu VM, Streisand JB, Polisson RP, Akesson A, Coppock J, van den Hoogen F, Herrick A, Mayes MD, Veale D, Seibold JR, Black CM, Korn JH. Scleroderma Clinical Trials Consortium. Validity, reliability, and feasibility of durometer measurements of scleroderma skin disease in a multicenter treatment trial. Arthritis Rheum 59, 699-705, 2008.

29) Morikawa H, Fukuda K, Kobayashi S, Fujii H, Iwai S, Enomoto M. Tamori A, Sakaguchi H, Kawada N. Real-time tissue elastography as a tool for the noninvasive assessment of liver stiffness in patients with chronic hepatitis C. J Gastroenterol 46, 350-358, 2011.

30) Morris MA, Ring CM, Managuli R, Saboury B, Mehregan, D, Siegel E, Dasgeb B. Feature analysis of ultrasound elastography image for quantitative assessment of cutaneous carcinoma. Skin Res Technol 24, 242-247, 2018.

31) Nakashima K, Shiina T, Sakurai M, Enokido K, Endo T, Tsunoda H, Takada E, Umemoto T, Ueno E. JSUM ultrasound elastography practice guidelines: breast. J Med Ultrason (2001) 40, 359-391, 2013.

32) Norlén L, Nicander I, Lundh Rozell B, Ollmar S, Forslind B. Inter- and intra-individual differences in human stratum corneum lipid content related to physical parameters of skin barrier function in vivo. J Invest Dermatol 112, 72-77, 1999.

33) Sim DJK, Kim SM, Kim SS, Doh I. Portable skin analyzers with simultaneous measurements of transepidermal water Loss, skin conductance and skin hardness. Sensors (Basel) 19, 3857, 2019.

34) Sim JK, Ahn B, Doh I. Truncated hollow cone probe for assessing transepidermal water loss and skin hardness. ACS Sens 3, 2246-2253, 2018.

35) Suehiro K, Nakamura K, Morikage N, Murakami M, Yamashita O, Ueda K, Samura M, Hamano K. Real-time tissue elastography assessment of skin and subcutaneous tissue strains in legs with lymphedema. J Med Ultrason 41, 359-364, 2014.

36) Tsui BCH, Tsui K. A flexible gel pad as an effective medium for scanning irregular surface anatomy. Can J Anesth 59, 226-227, 2012.

37) Xie L, Chen X, Guo Q, Dong Y, Guang Y, Zhang X. Real-time elastography for diagnosis of liver fibrosis in chronic hepatitis B. J Ultrasound Med Off J Am Inst Ultrasound Med 31, 1053-1060, 2012.

38) Yoon JH, Yoo J, Kim EK, Moon HJ, Lee HS, Seo JY, Park HY, Park WJ, Kwak JY. Real-time elastography in the evaluation of diffuse thyroid disease: a study based on elastography histogram parameters. Ultrasound Med Biol 40, 2012-2019, 2014.

39) Zhang Y, Tang J, Li Y, Fei X, Lv F, He E, Li Q, Shi H. Differentiation of prostate cancer from benign lesions using strain index of transrectal real-time tissue elastography. Eur J Radiol 81, 857-862, 2012.

40) Zhi H, Xiao XY, Yang HY, Ou B, Wen YL, Luo BM. Ultrasonic elastography in breast cancer diagnosis: Strain ratio vs 5-point scale. Acad Radiol 17, 1227-1233, 2010.